

# Order Matters: Exploring Order Sensitivity in Multimodal Large Language Models

Zhijie Tan<sup>1</sup>, Xu Chu<sup>1</sup>, Weiping Li<sup>1</sup>, Tong Mo<sup>1</sup>

<sup>1</sup>School of Software and Microelectronics, Peking University  
besttangent@stu.pku.edu.cn, chuxu@stu.pku.edu.cn, wpli@ss.pku.edu.cn, motong@ss.pku.edu.cn

## Abstract

Multimodal Large Language Models (MLLMs) utilize multimodal contexts consisting of text, images, or videos to solve various multimodal tasks. However, we find that changing the order of multimodal input can cause the model’s performance to fluctuate between advanced performance and random guessing. This phenomenon exists in both single-modality (text-only or image-only) and mixed-modality (image-text-pair) contexts. Furthermore, we demonstrate that popular MLLMs pay special attention to certain multimodal context positions, particularly the beginning and end. Leveraging this special attention, we place key video frames and important image/text content in special positions within the context and submit them to the MLLM for inference. This method results in average performance gains of 14.7% for video-caption matching and 17.8% for visual question answering tasks. Additionally, we propose a new metric, Position-Invariant Accuracy (PIA), to address order bias in MLLM evaluation. Our research findings contribute to a better understanding of Multi-Modal In-Context Learning (MMICL) and provide practical strategies for enhancing MLLM performance without increasing computational costs.

## Introduction

The recent success of Large Language Models (LLMs) (Zhao et al. 2023; Brown et al. 2020; Touvron et al. 2023; Bai et al. 2023a; Xi et al. 2024) has driven researchers to explore their capabilities in tackling multimodal tasks. By aligning image features with text embeddings, researchers integrate visual inputs into LLMs, developing Multimodal Large Language Models (MLLMs) (Yin et al. 2023; Li et al. 2023a; Alayrac et al. 2022; Li et al. 2023b; Beyer et al. 2024). These models inherit the exceptional abilities of LLMs in In-Context Learning (ICL) and have demonstrated significant performance in understanding and reasoning with images and videos.

A core issue in In-Context Learning for LLMs is prompt order. It has been shown in LLMs that there are better prompt orders (which vary between different models or tasks). When ordered correctly, the models perform well, whereas other orders result in performance close to random (Lu et al. 2021). The observation of prompt order sensitivity in LLMs raises two compelling questions. Question

Copyright © 2025, Association for the Advancement of Artificial Intelligence (www.aaai.org). All rights reserved.
















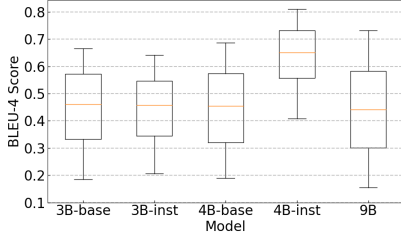
Question: Following the format of image-caption pairs, describe the final image.		
 The man has big black eyes and short eyelashes.	 A man with a broad chin and a square face.	 The man has big black eyes and short eyelashes.
 The lady has a melon seed face and a narrow chin.	 The lady has a melon seed face and a narrow chin.	 A man with a broad chin and a square face.
 An old man with a broad forehead.	 An old man with a broad forehead.	 An old man with a broad forehead.
 A man with a broad chin and a square face.	 The man has big black eyes and short eyelashes.	 The lady has a melon seed face and a narrow chin.
 ?	 ?	 ?
OpenFlamingo	OpenFlamingo	OpenFlamingo
Answer: A black hair man with short eyelashes. 😞 ❌	Answer: A man with a broad chin. 😞 ❌	Answer: A young woman with a round face and a narrow chin. 😊 ✅

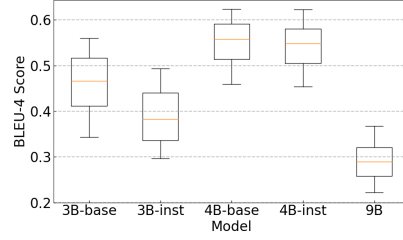
Figure 1: Certain multimodal context orders elicit accurate responses, while others lead to erroneous outputs. The green demonstration indicates good order, while the yellow and blue demonstrations indicate bad order.

I: “Does order sensitivity also exist in MLLMs?” Furthermore, another question that needs to be discussed is, Question II: “What kind of order is good for MLLM’s performance?” Current research and benchmark studies (Shi, Ma, and Vosoughi 2024; Chen et al. 2024; Liu et al. 2023b) focus on addressing a sub-question of Question I: “Does *text-only* order sensitivity also exist in MLLMs?”. These works overlook the potential influence of image order and situations where both image and text orders are altered.

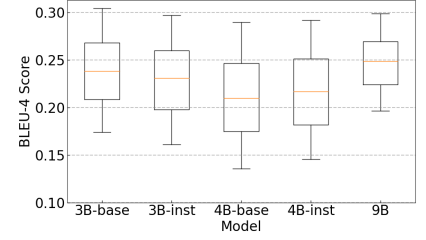
To fully answer Question I, we design the following experiments. As shown in Figure 1, CelebAText-HQ (Sun et al. 2021) is a facial image captioning dataset. We design a 4-shot image-text prompt and ask OpenFlamingo(Awadalla et al. 2023), a widely studied MLLM for multi-image input tasks (Yang et al. 2023; Chen et al. 2023a; Schlarman and Hein 2023), to generate a caption for a new facial image. When the image-text-pairs are arranged in good order (as illustrated in green in Figure 1), the model can generate essentially accurate responses. However, bad orders cause



(a) Text-only: Provide 4 images (different distinct views of the same facial image) and 4 corresponding captions, with the order of the captions randomly shuffled. The task for the model is to generate new captions.



(b) Image-only: Provide 4 images (different distinct views of the same facial image) and 4 corresponding captions, with the order of the images randomly shuffled. The task for the model is to generate new captions.



(c) Image-text-pair: Provide 4 images (facial images of 4 different persons) and 4 corresponding captions, with the order of the image-caption pairs randomly shuffled. The task for the model is to generate captions for a new facial image.

Figure 2: The performance of OpenFlamingo (Awadalla et al. 2023) (3B-base, 3B-instruct, 4B-base, 4B-instruct, 9B) with different multimodal context orders in the image captioning task.

the model’s responses to approach randomness (as shown in yellow and blue in Figure 1). Furthermore, as depicted in Figure 2, we demonstrate that altering the prompt order of text-only, image-only, or image-text-pair all impact the model’s performance in image captioning tasks. For text-only and image-only tasks, we employ HFGI3D (Xie et al. 2022) to generate four distinct views of each facial image as visual prompts. The detail of text-only and image-only tasks can be seen in Figure 10 and Figure 11 of Appendix A. The results indicate that both single-modality context order and mixed-modality context order significantly influence the model’s context learning performance. Moreover, we discover that high-performing prompts are not transferable across models. As shown in Figure 3, we utilize all 24 possible orderings of the 4-shot image-text prompts in the image-text-pair task. We then generate predictions using each prompt across different parameter versions of OpenFlamingo (Awadalla et al. 2023) and calculate pairwise Spearman rank correlation coefficients between the scores. The low correlations observed, such as  $-0.09$  between OpenFlamingo-3B-base and OpenFlamingo-4B-base, suggest that orderings beneficial for one model do not necessarily yield good performance in another. The degree of order sensitivity also varies among models. Figure 4 presents results from an image-caption matching task using modified COCO (Lin et al. 2014) dataset (for a detailed introduction, refer to the image-text-pair task in Figure 12 of Appendix B). It reveals that Qwen-VL-Chat-7B (Bai et al. 2023b) and DeepSeek-VL-7B (Lu et al. 2024) exhibit stronger order sensitivity for image-text-pairs compared to IDEFICS-9B-Instruct (Laurençon et al. 2023) and IDEFICS-v2-8B-Instruct (Laurençon et al. 2024). In summary, regarding Questions I, we believe that order sensitivity also exists in MLLMs, and changing the order of text-only, image-only, and image-text-pairs in the prompt all affect model performance. The magnitude of this impact varies for different models and different tasks.

Moreover, for Question II: “What kind of order is good for MLLM’s performance?” Previous research on prompt or-

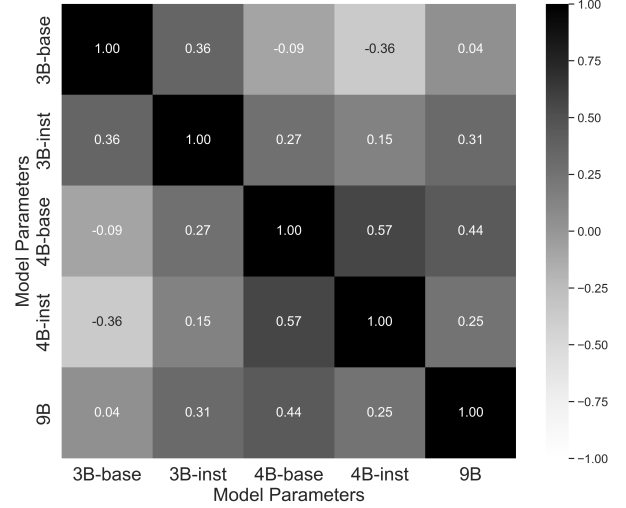


Figure 3: Spearman correlation coefficients of multimodal context order performance across OpenFlamingo models with varying parameter scales.

der in LLMs (Lu et al. 2021; Wu et al. 2022; Wang et al. 2023; Li et al. 2023d; Xu et al. 2023; Song et al. 2024) and our experiments on MLLMs both indicate that no universally optimal prompt order exists that generalizes well across different models and tasks. While many studies explore optimal prompt order (Lu et al. 2021; Wu et al. 2022; Yoo et al. 2021), they are often specific to certain modalities or tasks, making it difficult to extend these approaches to multimodal or universal tasks. Interestingly, considering that an order is composed of arrangements of different positions, we discover that popular MLLMs pay special attention to certain contextual positions, particularly the **beginning** and **end** of the input. As shown in Figure 5, in the image-caption matching task using the modified COCO dataset, placing the correct answer (image-text-pair) at the first and last options (*Op.A* and *Op.D*) results in the highest accuracy for all four

models. Conversely, placing the correct answer in the middle options (*Op.B* and *Op.C*) causes a significant drop in accuracy, with Qwen-VL-Chat-7B (Bai et al. 2023b) unable to provide the correct answer at all. This answers Question II: The order formed by placing important content at the beginning or end of the multimodal context is beneficial to the performance of popular MLLMs.

To utilize the order sensitivity to improve performance, we design two order-sensitive tasks for Multi-Modal In-Context Learning (MMICL): a video-caption matching task and a visual question answering task with Retrieval-Augmented Generation (RAG) (Lewis et al. 2020; Chen et al. 2022; Caffagni et al. 2024). In these experiments, we place keyframes of the video or important prompts in special positions within the multimodal context, demonstrating that this approach improves the accuracy of the model. This indicates that special positions in MLLMs contain rewards that can enhance the model’s capabilities. Additionally, we propose a new MLLM metric: Position-Invariant Accuracy (PIA). This metric aims to eliminate unfairness caused by order bias in models. PIA operates by cyclically placing the correct option in each position, then counting the number of times the model selects each option and the number of correct selections among them. Through weighted scoring, the essence of PIA is to reduce the bias introduced by the model’s tendency to favor certain options. We apply this metric to evaluate several widely studied and used MLLMs using the 4-option MMBench dataset (Liu et al. 2023b).

Our contributions are as follows:

- We demonstrate that order sensitivity exists in MLLMs, and changing the order of prompts can significantly affect the performance of MLLMs.
- We find that orders composed of some special positions are beneficial for MLLMs. Popular MLLMs pay special attention to the beginning and end of multimodal contexts. Placing important content in these positions can improve performance without additional computation.
- We prove that our finding on order sensitivity can be beneficial for order-dependent tasks such as video understanding and visual question answering, as demonstrated by our experiments on video-caption matching and visual question answering with RAG. The results show that using rewards for special positions in the context of understanding keyframes in videos and important prompts in RAG can improve model performance.
- We propose Position-Invariant Accuracy (PIA), a new MLLM metric designed to eliminate unfairness caused by order biases in MLLMs.

## Related Work

### Multimodal Large Language Model

Multimodal Large Language Model (MLLM) consist of pre-trained modality encoders, Large Language Models (LLMs), and modality alignment interfaces. Encoders like CLIP (Radford et al. 2021) use contrastive learning to align images and text for image-based tasks. Pre-trained LLMs (Ouyang et al. 2022; Bai et al. 2022; Touvron et al.

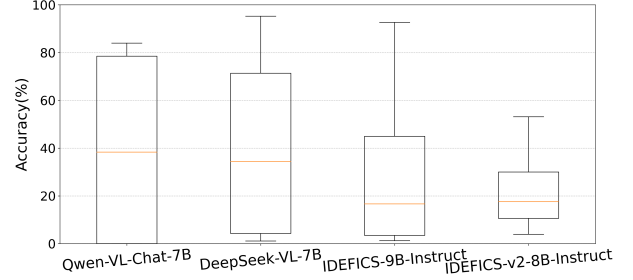


Figure 4: Performance of Qwen-VL-Chat-7B (Bai et al. 2023b), DeepSeek-VL-7B (Lu et al. 2024), IDEFICS-9B-Instruct (Laurençon et al. 2023) and IDEFICS-v2-8B-Instruct (Laurençon et al. 2024) on image captioning task for modified COCO dataset.

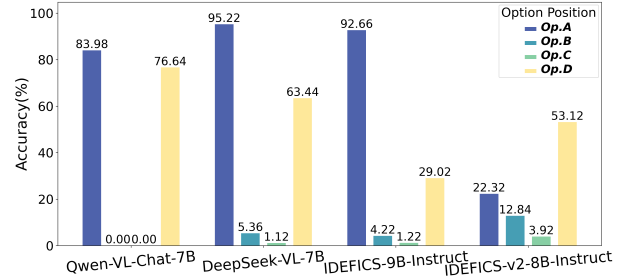


Figure 5: Performance of Qwen-VL-Chat-7B, DeepSeek-VL-7B, IDEFICS-9B-Instruct and IDEFICS-v2-8B-Instruct on image captioning task for modified COCO dataset, with different option positions.

2023), through extensive training on corpora, embed rich knowledge and exhibit strong generalization and reasoning capabilities. Modality alignment interfaces combine image-focused modality encoders with LLMs, which only understand text, to perform various multimodal tasks. The mainstream approach introduces learnable connectors between pre-trained modality encoders and LLMs. These connectors include learnable query tokens (e.g., BLIP-2 (Li et al. 2023a)), MLP (e.g., LLaVA (Liu et al. 2023a)), linear layer (e.g., PaliGemma (Beyer et al. 2024)), and the insertion of additional learnable modules (e.g., Flamingo (Alayrac et al. 2022), LLaMa-Adapter (Zhang et al. 2023a), and LLaVA-TokenPacker (Li et al. 2024)).

### Prompt Learning in MLLM

Prompt learning can be divided into hard prompts (discrete prompts) (Wen et al. 2023; Choi et al. 2024) and soft prompts (continuous prompts) (Qin and Eisner 2021; Wu et al. 2023). Hard prompts are typically composed of natural language words, making them easily understandable by humans. In contrast, soft prompts are usually learnable continuous vectors. Soft prompts are widely used in multimodal prompt learning, existing as continuous vectors in the embedding space of LLMs and being automatically learned during the fine-tuning process. CoOp (Zhou et al. 2021) fine-tunes CLIP by optimizing a set of continuous prompt vec-

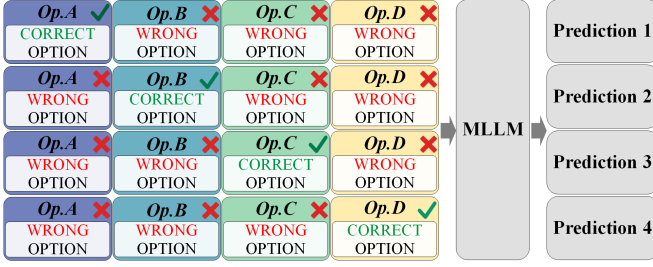


Figure 6: Evaluating the model’s performance by varying the position of the correct option within the multimodal context.

tors on its language branch to achieve a few-shot transfer. Additionally, many studies focus on optimizing prompts for single modalities in MLLM (Bahng et al. 2022; Ju et al. 2021; Lu et al. 2022). Unlike these works, Maple (Khatkhat et al. 2022) proposes a multimodal joint prompting method that couples prompts from both the language and image branches to fine-tune CLIP, achieving better results than single-modality prompting. ViLT-CLIP (Wang et al. 2024) introduces a method to reduce the discrepancy between hand-crafted prompts and learnable prompts, mitigating the forgetting of essential video scenarios and achieving the transfer of image-based CLIP to the video domain. ControlMLLM (Wu et al. 2024) dynamically adjusts visual-textual token interactions during inference, enabling precise regional descriptions and reasoning.

### Sensitivity of LLMs to Input Order

Jiang et al. (Jiang et al. 2019) find that LLMs are highly sensitive to the order of prompts in zero-shot and few-shot settings. Kumar and Talukdar explore finding the optimal order of training examples as enhanced prompts and learning delimiter tokens between prompts to further improve performance (Kumar and Talukdar 2021). Lu et al. (Lu et al. 2021) discover that the order in which response prompts are given to LLMs plays a crucial role in their performance and propose an entropy-based method to score different candidate orderings. Similarly, inspired by the learning compressed perspectives, Wu et al. (Wu et al. 2022) optimize the order by minimizing the encoding length required to compress and transmit test labels. Ma et al. (Ma et al. 2023) address the challenge of order in few-shot learning from the perspective of prediction bias. They introduce a greedy search strategy to identify the optimal prompt order. Zhang et al. (Zhang et al. 2024) tackle the order dependency in context learning by converting the n-shot problem into n parallel 1-shot tasks.

### Order Sensitivity

Previous research (Lu et al. 2021; Wu et al. 2022; Yoo et al. 2021) focuses on finding optimal orders for specific modalities and tasks. However, for a broader range of modalities and tasks, a general brute-force enumeration method for searching the optimal order requires unacceptable time consumption. Considering that an order is determined by the arrangement of different positions, we observe in extensive

experiments that popular MLLMs focus on specific positions within multimodal contexts. Therefore, our research focuses on utilizing these specific positions to construct better orders. In this section, we design three tasks to explore MLLM’s preferences for text-only positions, image-only positions, and image-text-pair positions. As shown in Figure 6, by altering the position of the correct option in the multimodal context and counting the times the model correctly answers questions at different positions, we assess the model’s position preference. Examples and descriptions of the three tasks are shown in Figure 12 of Appendix B.

### Text-only Order Sensitivity

We use the multiple-choice question-answering dataset MMBench (Liu et al. 2023b) to evaluate MLLM’s order preferences in text-only. Each question in this dataset contains an image and a question about the image, along with up to four text candidate options, with only one correct answer. For our experiments, we select questions with four candidate options and rotate the correct answer through the *Op.A*, *Op.B*, *Op.C*, and *Op.D* positions. The implementation details are as follows. Given question  $Q$  and the context input:

$$S_{\text{text-only}} = \{I; T_1; T_2; \dots; T_n\}, \quad (1)$$

where  $I$  represents the image on which question  $Q$  depends, and  $T_1; T_2; \dots; T_n$  represent the  $n$  text options, the model is required to answer question  $Q$  based on context  $S_{\text{text-only}}$  and choose the correct option from  $T_1; T_2; \dots; T_n$ .

In our experimental setup, we set  $n = 4$  and uniquely label the position of each text option as  $O_1 = (\text{Op.A}, T_1)$ ;  $O_2 = (\text{Op.B}, T_2)$ ;  $O_3 = (\text{Op.C}, T_3)$ ;  $O_4 = (\text{Op.D}, T_4)$ . We designate *Op.A* as the option representing the first position and *Op.D* as the option representing the last position. The context input is updated to:

$$S_{\text{text-only}} = \{I; O_1; O_2; O_3; O_4\}. \quad (2)$$

To explore the text-only order sensitivity of MLLM in In-Context Learning, we exchange the correct answer  $T_{\text{true}}$  with  $T_1, T_2, T_3$ , and  $T_4$  respectively, sequentially generating four variants of each question, and input them into the model in turn to obtain answers.

We conduct experiments on over 4,000 questions using IDEFICS-v2-8B-Instruct (Laurençon et al. 2024). To more clearly illustrate the impact of order on model performance, for each question, we exclude from the statistical data the results of questions that the model answers correctly in all four variants. We then tally the positions of the correct option when the model responds accurately. The results, shown in Figure 7(a), indicate that the model achieves the highest accuracy when the correct option is in position *Op.D* (i.e., the last option).

### Image-only Order Sensitivity

We use the COCO dataset (Lin et al. 2014) to create a multiple-choice image-caption matching task to evaluate MLLM’s order preferences in image-only. We select 5000 images with corresponding captions as correct answers. For each question, we add three random images as alternatives.



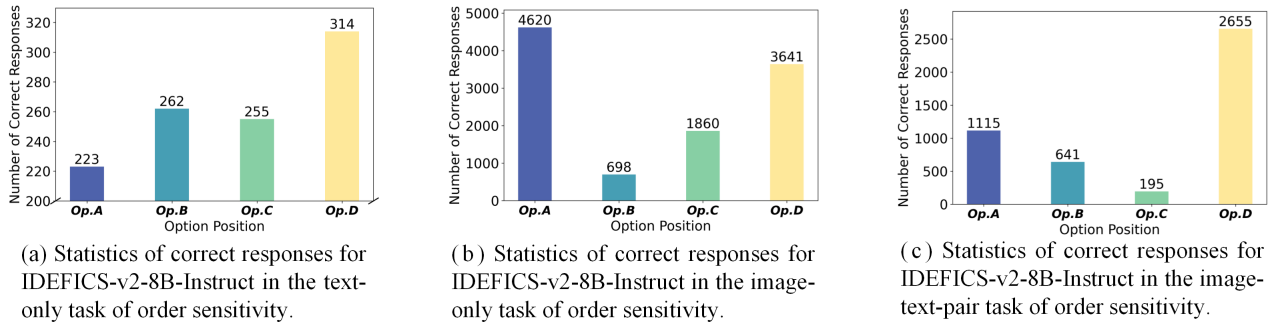


Figure 7: Statistics of correct responses for IDEFICS-v2-8B-Instruct (Laurençon et al. 2024) in order sensitivity tasks.

The task is to choose the image best matches the caption, with one correct answer. The correct answer in each question is sequentially swapped among the *Op.A*, *Op.B*, *Op.C*, and *Op.D* options. The implementation is as follows. Given question  $Q$  and the context input:

$$S_{\text{image-only}} = \{T; I_1; I_2; \dots; I_n\}, \quad (3)$$

where  $T$  represents the caption text, and  $I_1; I_2; \dots; I_n$  represent the  $n$  image options. The model is required to choose the image option that best matches the caption  $T$  from  $I_1; I_2; \dots; I_n$ .

In our experimental setup, we set  $n = 4$  and uniquely label the position of each image option as  $O_1 = (\text{Op.A}, I_1)$ ;  $O_2 = (\text{Op.B}, I_2)$ ;  $O_3 = (\text{Op.C}, I_3)$ ;  $O_4 = (\text{Op.D}, I_4)$ . We designate *Op.A* as the option representing the first position and *Op.D* as the option representing the last position. The context input is updated to:

$$S_{\text{image-only}} = \{T; O_1; O_2; O_3; O_4\}. \quad (4)$$

To explore the image-only order sensitivity of MLLM in In-Context Learning, we exchange the correct answer  $I_{\text{true}}$  with each of  $I_1; I_2; I_3; I_4$  respectively, sequentially generating four variants of each question, and input them into the model in turn to obtain answers.

We conduct experiments on 5,000 questions using IDEFICS-v2-8B-Instruct (Laurençon et al. 2024). To more clearly illustrate the impact of order on model performance, for each question, we exclude from the statistical data the results of questions that the model answers correctly in all four variants. We then tally the positions of the correct option when the model responds accurately. The results, shown in Figure 7(b), indicate that the model’s accuracy is highest when the correct answer is in position *Op.A* or *Op.D* (the first or last option).

### Mixed-modality Order Sensitivity

We utilize the COCO dataset (Lin et al. 2014) to construct a multiple-choice image-caption matching task to evaluate MLLM’s order preferences for mixed modalities (image-text-pairs). We select 5000 image-caption pairs as correct answers. For each question, we add three random image-caption pairs as alternatives. The task is to choose the best matching pair, with one correct answer. The correct option in each question is sequentially swapped among the *Op.A*,

*Op.B*, *Op.C*, and *Op.D* options. The implementation is as follows. Given question  $Q$  and the context input:

$$S_{\text{image-text-pair}} = \{(I_1, T_1); (I_2, T_2); \dots; (I_n, T_n)\}, \quad (5)$$

where  $(I_1, T_1); (I_2, T_2); \dots; (I_n, T_n)$  represent  $n$  image-text-pairs. The model is required to choose the most matching image and caption pair from  $(I_1, T_1); (I_2, T_2); \dots; (I_n, T_n)$ .

In our experimental setup, we set  $n = 4$  and label each image-text-pair option with a unique position, namely  $O_1 = (\text{Op.A}, (I_1, T_1))$ ;  $O_2 = (\text{Op.B}, (I_2, T_2))$ ;  $O_3 = (\text{Op.C}, (I_3, T_3))$ ;  $O_4 = (\text{Op.D}, (I_4, T_4))$ . We designate *Op.A* as the option representing the first position and *Op.D* as the option representing the last position. The context input is updated to:

$$S_{\text{image-text-pair}} = \{O_1; O_2; O_3; O_4\}. \quad (6)$$

To explore the mixed-modality order sensitivity of MLLM in In-Context Learning, we exchange the correct answer  $(I, T)_{\text{true}}$  with each of  $(I_1, T_1); (I_2, T_2); (I_3, T_3); (I_4, T_4)$  respectively, sequentially generating four variants of each question, and input them into the model in turn to obtain answers.

We experiment with 5,000 questions using IDEFICS-v2-8B-Instruct (Laurençon et al. 2024). To more clearly illustrate the impact of order on model performance, for each question, we exclude from the statistical data the results of questions that the model answers correctly in all four variants. We then tally the positions of the correct option when the model responds accurately. Figure 7(c) shows the model’s accuracy is highest when the correct answer is positioned in *Op.A* or *Op.D* (first or last option).

Model	Parameters	Tokens Per Image
DeepSeek-VL	7B	576
LLaVa-NeXT	7B/13B/34B	2880
IDEFICS-v2	8B	320
MM1-Chat	7B/30B	720

Table 1: Tokens per image in DeepSeek-VL (Lu et al. 2024), LLaVa-NeXT (Liu et al. 2023a), IDEFICS-v2 (Laurençon et al. 2024), and MM1-Chat (McKinzie et al. 2024).

## Analysis

The experimental results indicate that MLLMs prefer the beginning and end of the multimodal context. When the correct answer is positioned at the beginning or end, the model’s chances of accurately answering the question increase. Even if the model cannot answer the question correctly, it tends to rely on the beginning and end of the context for its response. This phenomenon is more pronounced in image-only or mixed-modality tasks than in text-only tasks. The token length of encoded images is closer to that of long texts, as shown in Table 1. This suggests that order bias may relate to the context length, with longer text lengths potentially amplifying this effect.

These results inspire us to consider: Would tasks influenced by order, such as video understanding and visual question answering (when visual prompts have an order), benefit from orders composed of these special positions? In the next section, we design two experiments: a video-caption matching task and a visual question answering task with RAG, to demonstrate the impact of prompt orders composed of special positions on these tasks.

## Experiment

### Settings

We use Video-LLaVA (Lin et al. 2023) for the video-caption matching task and IDEFICS-v2-8B-Instruct (Laurençon et al. 2024) for the visual question answering task with Retrieval-Augmented Generation (RAG). The experimental setup can be seen in Appendix C.

### Dataset

**Video-Caption Matching.** Task construction is shown in Figure 13 of Appendix C. The MVBench (Li et al. 2023c) dataset serves as the foundation. MVBench is a commonly used dataset for MLLM instruction fine-tuning (Li et al. 2023b; Zhang, Li, and Bing 2023), containing multiple tasks and video collections. We focus on the fine-grained pose video set, comprising 200 fine-grained action video clips with corresponding textual captions. Our selection criteria include action lengths between 2-3 seconds (135 video clips), which we extend to create new 10-second videos. In each new video, we designate the original 2-3 second clip as the key action and randomly sample other action clips, concatenating them sequentially until reaching 10 seconds. Each video pairs with a caption-matching question: “Is anyone in the video performing the following action: action?” where “action” represents the textual caption of the key action. The model needs to answer with “Yes” or “No”.

The video frames corresponding to the key action are referred to as *Key Frames* (as the frames within the green boxes in Figure 13). For each video, we construct three comparative groups: we move *Key Frames* to the front, middle, and back, respectively, resulting in three new videos with different arrangements of *Key Frames*. The corresponding question and answer for each video remain unchanged.

**Visual Question Answering with RAG.** Task construction can be seen in Figure 14 of Appendix C. The multiple-choice question-answering dataset MMbench (Liu et al.

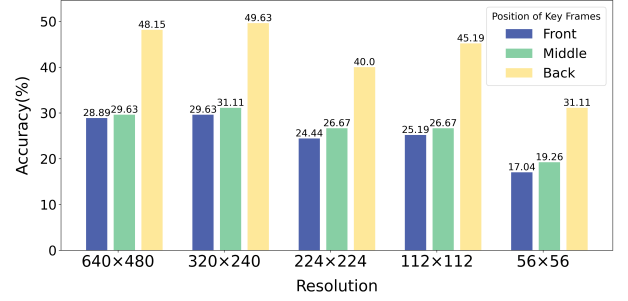


Figure 8: Statistics of correct responses for Video-LLaVA in video-caption matching task.

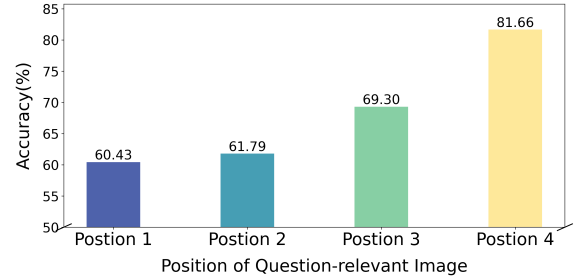


Figure 9: Statistics of correct responses for IDEFICS-v2-8B-Instruct in question-answering task with RAG.

2023b) serves as the foundation for our construction. Each question in MMbench includes an image and a question about the image, along with up to 4 textual candidate options, with only one correct answer. To simulate RAG results, for each question, we refer to the image corresponding to the question as the *Question-relevant image* (as the image within the green boxes in Figure 14), and randomly select 3 other questions, obtaining their corresponding images. We combine these 4 images to form a RAG image set, in which only 1 image is relevant to the question, namely the *Question-relevant image*. In our newly constructed dataset, each entry includes a RAG image set, a question about the *Question-relevant image*, and four text candidate options.

For each question, we create four comparative groups by positioning the *Question-relevant image* in the first, second, third, and fourth positions within the RAG image set, respectively. The question and answer for each entry remain consistent across all groups.

**Position-Invariant Accuracy.** We select questions with four options from the multiple-choice question-answering dataset MMbench (Liu et al. 2023b), referred to as the 4-option MMbench dataset. To calculate Position-Invariant Accuracy, for each question, we place the correct option in *Op.A*, *Op.B*, *Op.C*, and *Op.D* respectively to create four comparison groups.

## Results

**Video-Caption Matching.** We set the frame sampling number to 15, ensuring the key action is sampled in all three comparative experiments. Figure 8 shows the experimen-

Model	Parameters	Accuracy (%)	Circular Evaluation Accuracy (%)	Position-Invariant Accuracy (PIA) (%)
InternLM-XComposer2 (Dong et al. 2024)	1.8B	76.11	69.74	57.66
Qwen-VL-Chat (Bai et al. 2023b)	7B	71.84	55.83	53.30
DeepSeek-VL (Lu et al. 2024)	7B	80.13	73.89	64.24
IDEFICS-v2 (Laurençon et al. 2024)	8B	83.86	76.94	70.18
InternVL-Chat-v1.5 (Chen et al. 2023b)	26B	84.90	79.27	71.38
EMU2-Chat (Sun et al. 2023)	37B	76.35	65.00	58.89

Table 2: Performance of different MLLMs on the 4-option MMBench dataset.

tal results. Our independent repeated experiments conducted under 5 video resolutions ( $640 \times 480$ ,  $320 \times 240$ ,  $224 \times 224$ ,  $112 \times 112$ , and  $56 \times 56$ ) indicate that, regardless of the resolution, placing the *Key Frames* at the back of the video yields the highest model accuracy, despite the same key action appearing in all three comparative experiments. Compared to positioning the *Key Frames* at the beginning and middle, the average accuracy improves by 17.78% and 16.15% respectively across the 5 resolutions.

**Visual Question Answering with RAG.** Figure 9 shows the experimental results. Although all four comparative groups contain the *Question-relevant image*, positioning the *Question-relevant image* in the last position of the RAG image set produces the highest model accuracy. Compared to the first three positions, the accuracy increases by 21.23%, 19.87%, and 12.36%, respectively.

**Position-Invariant Accuracy.** Existing MLLM benchmarks overlook the model’s sensitivity to order, where altering the correct answer’s position can significantly impact model performance. Liu et al. (Liu et al. 2023b) introduce the Circular Evaluation Strategy to address this issue. In this approach, the correct answer is cyclically shifted across  $M$  options and evaluated  $M$  times, with the problem considered solved only if the model succeeds in all  $M$  trials. However, this metric primarily assesses model robustness and fails to eliminate the inherent unfairness caused by order bias during evaluation. Consider a scenario where a model exhibits a strong tendency to select *Op.A* with high frequency. In this case, choosing the correct option *Op.A* might stem from this bias rather than true understanding, suggesting that a lower scoring weight should be applied to mitigate this tendency. Conversely, if the model rarely selects *Op.B*, choosing the correct option *Op.B* indicates high confidence and should be accorded a higher scoring weight.

To address these nuances, we propose a novel metric: Position-Invariant Accuracy (PIA). This metric is designed to account for and neutralize order biases in model responses, offering a more equitable evaluation of MLLM performance. The PIA is defined as follows:

$$\text{PIA} = \frac{1}{M} \sum_{i=1}^M \frac{C_i}{Pr_i} \cdot \frac{C_i}{N}, \quad (7)$$

where  $M$  represents the number of options,  $C_i$  denotes the total number of times the model correctly answers the  $i$ -th option,  $Pr_i$  represents the total number of times the model selects the  $i$ -th option, and  $N$  represents the total number

of questions in the dataset before constructing the comparison groups.  $\frac{C_i}{Pr_i}$  indicates the extent to which the model’s selection of option  $i$  is due to its order bias. PIA assigns lower-scoring weights to the model’s preferred positions and higher-scoring weights to its less preferred positions, thereby mitigating the unfairness caused by order bias in the evaluation results.

To demonstrate the effectiveness of PIA, as shown in Table 2, we evaluate the accuracy, Circular Evaluation Accuracy, and Position-Invariant Accuracy (PIA) of 6 widely studied and used MLLMs on the 4-option MMBench dataset. The results show that PIA is smaller than both accuracy and Circular Evaluation Accuracy. This is due to its scaling factor  $\frac{C_i}{Pr_i}$ , which penalizes the MLLM’s tendency to blindly choose *Op.A* or *Op.D*.

## Future Work & Conclusion

The impact of order sensitivity on MLLM’s performance is significant, with models often favoring the beginning and end of multimodal context. We believe this reflects human cognitive behavior - when the context is long, people tend to forget the middle content and focus on the beginning and end. The implications of this finding are twofold. Firstly, prompting techniques like Multi-Modal In-Context Learning (MMICL) (Khattak et al. 2022; Wang et al. 2024; Wu et al. 2024) and Chain of Thought (CoT) (Wei et al. 2022; Zhang et al. 2023b; Mitra et al. 2024) heavily rely on prompt order, making it necessary to re-examine the design of these tasks given the discovery of order sensitivity. Secondly, designing or training models also needs to pay more attention to order sensitivity. This is because current training data and task construction may inherently carry biases, with questions typically positioned at the beginning and end of context. This phenomenon calls for more diverse data and tasks.

In this paper, we demonstrate that MLLMs exhibit order sensitivity and find prompt orders that can improve performance. Popular MLLMs show a preference for the beginning and end of multimodal contexts, and placing important content in these positions can enhance performance. This is beneficial for improving accuracy in order-sensitive tasks such as video understanding and visual question answering. Finally, we propose a new MLLM metric: Position Invariant Accuracy (PIA), mitigating the unfair impact of order preferences.

## References

- Alayrac, J.-B.; Donahue, J.; Luc, P.; Miech, A.; Barr, I.; Hasson, Y.; Lenc, K.; Mensch, A.; Millican, K.; Reynolds, M.; Ring, R.; Rutherford, E.; Cabi, S.; Han, T.; Gong, Z.; Samangooei, S.; Monteiro, M.; Menick, J.; Borgeaud, S.; Brock, A.; Nematzadeh, A.; Sharifzadeh, S.; Binkowski, M.; Barreira, R.; Vinyals, O.; Zisserman, A.; and Simonyan, K. 2022. Flamingo: a Visual Language Model for Few-Shot Learning. *ArXiv*, abs/2204.14198.
- Awadalla, A.; Gao, I.; Gardner, J.; Hessel, J.; Hanafy, Y.; Zhu, W.; Marathe, K.; Bitton, Y.; Gadre, S. Y.; Sagawa, S.; Jitsev, J.; Kornblith, S.; Koh, P. W.; Ilharco, G.; Wortsman, M.; and Schmidt, L. 2023. OpenFlamingo: An Open-Source Framework for Training Large Autoregressive Vision-Language Models. *ArXiv*, abs/2308.01390.
- Bahng, H.; Jahanian, A.; Sankaranarayanan, S.; and Isola, P. 2022. Visual Prompting: Modifying Pixel Space to Adapt Pre-trained Models. *ArXiv*, abs/2203.17274.
- Bai, J.; Bai, S.; Chu, Y.; Cui, Z.; Dang, K.; Deng, X.; Fan, Y.; Ge, W.; Han, Y.; Huang, F.; Hui, B.; Ji, L.; Li, M.; Lin, J.; Lin, R.; Liu, D.; Liu, G.; Lu, C.; Lu, K.; Ma, J.; Men, R.; Ren, X.; Ren, X.; Tan, C.; Tan, S.; Tu, J.; Wang, P.; Wang, S.; Wang, W.; Wu, S.; Xu, B.; Xu, J.; Yang, A.; Yang, H.; Yang, J.; Yang, S.; Yao, Y.; Yu, B.; Yuan, H.; Yuan, Z.; Zhang, J.; Zhang, X.; Zhang, Y.; Zhang, Z.; Zhou, C.; Zhou, J.; Zhou, X.; and Zhu, T. 2023a. Qwen Technical Report. *arXiv preprint arXiv:2309.16609*.
- Bai, J.; Bai, S.; Yang, S.; Wang, S.; Tan, S.; Wang, P.; Lin, J.; Zhou, C.; and Zhou, J. 2023b. Qwen-VL: A Frontier Large Vision-Language Model with Versatile Abilities. *arXiv preprint arXiv:2308.12966*.
- Bai, Y.; Kadavath, S.; Kundu, S.; Askell, A.; Kernion, J.; Jones, A.; Chen, A.; Goldie, A.; Mirhoseini, A.; McKinnon, C.; Chen, C.; Olsson, C.; Olah, C.; Hernandez, D.; Drain, D.; Ganguli, D.; Li, D.; Tran-Johnson, E.; Perez, E.; Kerr, J.; Mueller, J.; Ladish, J.; Landau, J.; Ndousse, K.; Lukošiušė, K.; Lovitt, L.; Sellitto, M.; Elhage, N.; Schiefer, N.; Mercado, N.; DasSarma, N.; Lasenby, R.; Larson, R.; Ringer, S.; Johnston, S.; Kravec, S.; Showk, S. E.; Fort, S.; Lanham, T.; Telleen-Lawton, T.; Conerly, T.; Henighan, T.; Hume, T.; Bowman, S.; Hatfield-Dodds, Z.; Mann, B.; Amodei, D.; Joseph, N.; McCandlish, S.; Brown, T. B.; and Kaplan, J. 2022. Constitutional AI: Harmlessness from AI Feedback. *ArXiv*, abs/2212.08073.
- Beyer, L.; Steiner, A.; Pinto, A. S.; Kolesnikov, A.; Wang, X.; Salz, D.; Neumann, M.; Alabdulmohsin, I.; Tschannen, M.; Bugliarello, E.; et al. 2024. PaliGemma: A versatile 3B VLM for transfer. *arXiv preprint arXiv:2407.07726*.
- Brown, T. B.; Mann, B.; Ryder, N.; Subbiah, M.; Kaplan, J.; Dhariwal, P.; Neelakantan, A.; Shyam, P.; Sastry, G.; Askell, A.; Agarwal, S.; Herbert-Voss, A.; Krueger, G.; Henighan, T.; Child, R.; Ramesh, A.; Ziegler, D. M.; Wu, J.; Winter, C.; Hesse, C.; Chen, M.; Sigler, E.; teusz Litwin, M.; Gray, S.; Chess, B.; Clark, J.; Berner, C.; McCandlish, S.; Radford, A.; Sutskever, I.; and Amodei, D. 2020. Language Models are Few-Shot Learners. *ArXiv*, abs/2005.14165.
- Caffagni, D.; Cocchi, F.; Moratelli, N.; Sarto, S.; Cornia, M.; Baraldi, L.; and Cucchiara, R. 2024. Wiki-LLaVA: Hierarchical Retrieval-Augmented Generation for Multimodal LLMs. In *Proceedings of the IEEE/CVF Conference on Computer Vision and Pattern Recognition*, 1818–1826.
- Chen, D.; Chen, R.; Zhang, S.; Liu, Y.; Wang, Y.; Zhou, H.; Zhang, Q.; Zhou, P.; Wan, Y.; and Sun, L. 2024. Mllm-as-a-judge: Assessing multimodal llm-as-a-judge with vision-language benchmark. *arXiv preprint arXiv:2402.04788*.
- Chen, D.; Liu, J.; Dai, W.; and Wang, B. 2023a. Visual Instruction Tuning with Polite Flamingo. In *AAAI Conference on Artificial Intelligence*.
- Chen, W.; Hu, H.; Chen, X.; Verga, P.; and Cohen, W. W. 2022. MuRAG: Multimodal Retrieval-Augmented Generator for Open Question Answering over Images and Text. In *Conference on Empirical Methods in Natural Language Processing*.
- Chen, Z.; Wu, J.; Wang, W.; Su, W.; Chen, G.; Xing, S.; Zhong, M.; Zhang, Q.; Zhu, X.; Lu, L.; Li, B.; Luo, P.; Lu, T.; Qiao, Y.; and Dai, J. 2023b. InternVL: Scaling up Vision Foundation Models and Aligning for Generic Visual-Linguistic Tasks. *arXiv preprint arXiv:2312.14238*.
- Choi, Y.; Bae, S.; Ban, S.; Jeong, M.; Zhang, C.; Song, L.; Zhao, L.; Bian, J.; and Kim, K.-E. 2024. Hard Prompts Made Interpretable: Sparse Entropy Regularization for Prompt Tuning with RL. *arXiv preprint arXiv:2407.14733*.
- Dong, X.; Zhang, P.; Zang, Y.; Cao, Y.; Wang, B.; Ouyang, L.; Wei, X.; Zhang, S.; Duan, H.; Cao, M.; Zhang, W.; Li, Y.; Yan, H.; Gao, Y.; Zhang, X.; Li, W.; Li, J.; Chen, K.; He, C.; Zhang, X.; Qiao, Y.; Lin, D.; and Wang, J. 2024. InternLM-XComposer2: Mastering Free-form Text-Image Composition and Comprehension in Vision-Language Large Model. *arXiv preprint arXiv:2401.16420*.
- Jiang, Z.; Xu, F. F.; Araki, J.; and Neubig, G. 2019. How Can We Know What Language Models Know? *Transactions of the Association for Computational Linguistics*, 8: 423–438.
- Ju, C.; Han, T.; Zheng, K.; Zhang, Y.; and Xie, W. 2021. Prompting Visual-Language Models for Efficient Video Understanding. In *European Conference on Computer Vision*.
- Khattak, M. U.; Rasheed, H. A.; Maaz, M.; Khan, S. H.; and Khan, F. S. 2022. MaPLe: Multi-modal Prompt Learning. *2023 IEEE/CVF Conference on Computer Vision and Pattern Recognition (CVPR)*, 19113–19122.
- Kumar, S.; and Talukdar, P. P. 2021. Reordering Examples Helps during Priming-based Few-Shot Learning. In *Findings*.
- Laurençon, H.; Saulnier, L.; Tronchon, L.; Bekman, S.; Singh, A.; Lozhkov, A.; Wang, T.; Karamcheti, S.; Rush, A. M.; Kiela, D.; Cord, M.; and Sanh, V. 2023. OBELICS: An Open Web-Scale Filtered Dataset of Interleaved Image-Text Documents. *arXiv:2306.16527*.
- Laurençon, H.; Tronchon, L.; Cord, M.; and Sanh, V. 2024. What matters when building vision-language models? *ArXiv*, abs/2405.02246.
- Lewis, P.; Perez, E.; Piktus, A.; Petroni, F.; Karpukhin, V.; Goyal, N.; Küttler, H.; Lewis, M.; Yih, W.-t.; Rocktäschel, T.; et al. 2020. Retrieval-augmented generation for



- knowledge-intensive nlp tasks. *Advances in Neural Information Processing Systems*, 33: 9459–9474.
- Li, J.; Li, D.; Savarese, S.; and Hoi, S. C. H. 2023a. BLIP-2: Bootstrapping Language-Image Pre-training with Frozen Image Encoders and Large Language Models. In *International Conference on Machine Learning*.
- Li, K.; He, Y.; Wang, Y.; Li, Y.; Wang, W.; Luo, P.; Wang, Y.; Wang, L.; and Qiao, Y. 2023b. VideoChat: Chat-Centric Video Understanding. *ArXiv*, abs/2305.06355.
- Li, K.; Wang, Y.; He, Y.; Li, Y.; Wang, Y.; Liu, Y.; Wang, Z.; Xu, J.; Chen, G.; Luo, P.; Wang, L.; and Qiao, Y. 2023c. MVBench: A Comprehensive Multi-modal Video Understanding Benchmark. *ArXiv*, abs/2311.17005.
- Li, W.; Yuan, Y.; Liu, J.; Tang, D.; Wang, S.; Zhu, J.; and Zhang, L. 2024. TokenPacker: Efficient Visual Projector for Multimodal LLM. *ArXiv*, abs/2407.02392.
- Li, Z.; Wang, C.; Ma, P.; Wu, D.; Li, T.; Wang, S.; Gao, C.; and Liu, Y. 2023d. Split and Merge: Aligning Position Biases in Large Language Model based Evaluators. *ArXiv*, abs/2310.01432.
- Lin, B.; Zhu, B.; Ye, Y.; Ning, M.; Jin, P.; and Yuan, L. 2023. Video-LLaVA: Learning United Visual Representation by Alignment Before Projection. *ArXiv*, abs/2311.10122.
- Lin, T.-Y.; Maire, M.; Belongie, S. J.; Hays, J.; Perona, P.; Ramanan, D.; Dollár, P.; and Zitnick, C. L. 2014. Microsoft COCO: Common Objects in Context. In *European Conference on Computer Vision*.
- Liu, H.; Li, C.; Wu, Q.; and Lee, Y. J. 2023a. Visual Instruction Tuning. In *NeurIPS*.
- Liu, Y.; Duan, H.; Zhang, Y.; Li, B.; Zhang, S.; Zhao, W.; Yuan, Y.; Wang, J.; He, C.; Liu, Z.; Chen, K.; and Lin, D. 2023b. MMBench: Is Your Multi-modal Model an All-around Player? *ArXiv*, abs/2307.06281.
- Lu, H.; Liu, W.; Zhang, B.; Wang, B.; Dong, K.; Liu, B.; Sun, J.; Ren, T.; Li, Z.; Yang, H.; Sun, Y.; Deng, C.; Xu, H.; Xie, Z.; and Ruan, C. 2024. DeepSeek-VL: Towards Real-World Vision-Language Understanding. *arXiv:2403.05525*.
- Lu, Y.; Bartolo, M.; Moore, A.; Riedel, S.; and Stenetorp, P. 2021. Fantastically Ordered Prompts and Where to Find Them: Overcoming Few-Shot Prompt Order Sensitivity. *ArXiv*, abs/2104.08786.
- Lu, Y.; Liu, J.; Zhang, Y.; Liu, Y.; and Tian, X. 2022. Prompt Distribution Learning. *2022 IEEE/CVF Conference on Computer Vision and Pattern Recognition (CVPR)*, 5196–5205.
- Ma, H.; Zhang, C.; Bian, Y.; Liu, L.; Zhang, Z.; Zhao, P.; Zhang, S.; Fu, H.; Hu, Q.; and Wu, B. 2023. Fairness-guided Few-shot Prompting for Large Language Models. *ArXiv*, abs/2303.13217.
- McKinzie, B.; Gan, Z.; Fauconnier, J.-P.; Dodge, S.; Zhang, B.; Dufter, P.; Shah, D.; Du, X.; Peng, F.; Weers, F.; Belyi, A.; Zhang, H.; Singh, K.; Kang, D.; Jain, A.; He, H.; Schwarzer, M.; Gunter, T.; Kong, X.; Zhang, A.; Wang, J.; Wang, C.; Du, N.; Lei, T.; Wiseman, S.; Yin, G.; Lee, M.; Wang, Z.; Pang, R.; Gräsch, P.; Toshev, A.; and Yang, Y. 2024. MM1: Methods, Analysis & Insights from Multi-modal LLM Pre-training. *ArXiv*, abs/2403.09611.
- Mitra, C.; Huang, B.; Darrell, T.; and Herzig, R. 2024. Compositional chain-of-thought prompting for large multimodal models. In *Proceedings of the IEEE/CVF Conference on Computer Vision and Pattern Recognition*, 14420–14431.
- Ouyang, L.; Wu, J.; Jiang, X.; Almeida, D.; Wainwright, C. L.; Mishkin, P.; Zhang, C.; Agarwal, S.; Slama, K.; Ray, A.; Schulman, J.; Hilton, J.; Kelton, F.; Miller, L. E.; Simens, M.; Askell, A.; Welinder, P.; Christiano, P. F.; Leike, J.; and Lowe, R. J. 2022. Training language models to follow instructions with human feedback. *ArXiv*, abs/2203.02155.
- Qin, G.; and Eisner, J. 2021. Learning how to ask: Querying LMs with mixtures of soft prompts. *arXiv preprint arXiv:2104.06599*.
- Radford, A.; Kim, J. W.; Hallacy, C.; Ramesh, A.; Goh, G.; Agarwal, S.; Sastry, G.; Askell, A.; Mishkin, P.; Clark, J.; Krueger, G.; and Sutskever, I. 2021. Learning Transferable Visual Models From Natural Language Supervision. In *International Conference on Machine Learning*.
- Schlarman, C.; and Hein, M. 2023. On the adversarial robustness of multi-modal foundation models. In *Proceedings of the IEEE/CVF International Conference on Computer Vision*, 3677–3685.
- Shi, L.; Ma, W.; and Vosoughi, S. 2024. Judging the Judges: A Systematic Investigation of Position Bias in Pairwise Comparative Assessments by LLMs. *arXiv preprint arXiv:2406.07791*.
- Song, W.; Oh, S.; Mo, S.; Kim, J.; Yun, S.; Ha, J.-W.; and Shin, J. 2024. Hierarchical Context Merging: Better Long Context Understanding for Pre-trained LLMs. *ArXiv*, abs/2404.10308.
- Sun, J.; Li, Q.; Wang, W.; Zhao, J.; and Sun, Z. 2021. Multi-caption Text-to-Face Synthesis: Dataset and Algorithm. *Proceedings of the 29th ACM International Conference on Multimedia*.
- Sun, Q.; Cui, Y.; Zhang, X.; Zhang, F.; Yu, Q.; Luo, Z.; Wang, Y.; Rao, Y.; Liu, J.; Huang, T.; and Wang, X. 2023. Generative Multimodal Models are In-Context Learners. *ArXiv*, abs/2312.13286.
- Touvron, H.; Lavril, T.; Izacard, G.; Martinet, X.; Lachaux, M.-A.; Lacroix, T.; Rozière, B.; Goyal, N.; Hambro, E.; Azhar, F.; Rodriguez, A.; Joulin, A.; Grave, E.; and Lample, G. 2023. LLaMA: Open and Efficient Foundation Language Models. *ArXiv*, abs/2302.13971.
- Wang, H.; Liu, F.; Jiao, L.; Wang, J.; Hao, Z.; Li, S.; Li, L.; Chen, P.; and Liu, X. 2024. ViLT-CLIP: Video and Language Tuning CLIP with Multimodal Prompt Learning and Scenario-Guided Optimization. In *AAAI Conference on Artificial Intelligence*.
- Wang, P.; Li, L.; Chen, L.; Zhu, D.; Lin, B.; Cao, Y.; Liu, Q.; Liu, T.; and Sui, Z. 2023. Large Language Models are not Fair Evaluators. *ArXiv*, abs/2305.17926.
- Wei, J.; Wang, X.; Schuurmans, D.; Bosma, M.; Xia, F.; Chi, E.; Le, Q. V.; Zhou, D.; et al. 2022. Chain-of-thought prompting elicits reasoning in large language models. *Advances in neural information processing systems*, 35: 24824–24837.

Wen, Y.; Jain, N.; Kirchenbauer, J.; Goldblum, M.; Geiping, J.; and Goldstein, T. 2023. Hard Prompts Made Easy: Gradient-Based Discrete Optimization for Prompt Tuning and Discovery. *ArXiv*, abs/2302.03668.

Wu, J.; Yu, T.; Wang, R.; Song, Z.; Zhang, R.; Zhao, H.; Lu, C.; Li, S.; and Henao, R. 2023. InfoPrompt: Information-Theoretic Soft Prompt Tuning for Natural Language Understanding. *ArXiv*, abs/2306.04933.

Wu, M.; Cai, X.; Ji, J.; Li, J.; Huang, O.; Luo, G.; Fei, H.; Sun, X.; and Ji, R. 2024. ControlMLLM: Training-Free Visual Prompt Learning for Multimodal Large Language Models. *arXiv preprint arXiv:2407.21534*.

Wu, Z.; Wang, Y.; Ye, J.; and Kong, L. 2022. Self-Adaptive In-Context Learning: An Information Compression Perspective for In-Context Example Selection and Ordering. In *Annual Meeting of the Association for Computational Linguistics*.

Xi, Z.; Chen, W.; Hong, B.; Jin, S.; Zheng, R.; He, W.; Ding, Y.; Liu, S.; Guo, X.; Wang, J.; Guo, H.; Shen, W.; Fan, X.; Zhou, Y.; Dou, S.; Wang, X.; Zhang, X.; Sun, P.; Gui, T.; Zhang, Q.; and Huang, X. 2024. Training Large Language Models for Reasoning through Reverse Curriculum Reinforcement Learning. *ArXiv*, abs/2402.05808.

Xie, J.; Ouyang, H.; Piao, J.; Lei, C.; and Chen, Q. 2022. High-fidelity 3D GAN Inversion by Pseudo-multi-view Optimization. *2023 IEEE/CVF Conference on Computer Vision and Pattern Recognition (CVPR)*, 321–331.

Xu, P.; Ping, W.; Wu, X.; McAfee, L. C.; Zhu, C.; Liu, Z.; Subramanian, S.; Bakhturina, E.; Shoenybi, M.; and Catanzaro, B. 2023. Retrieval meets Long Context Large Language Models. *ArXiv*, abs/2310.03025.

Yang, X.; Wu, Y.; Yang, M.-H.; Chen, H.; and Geng, X. 2023. Exploring Diverse In-Context Configurations for Image Captioning. *ArXiv*, abs/2305.14800.

Yin, S.; Fu, C.; Zhao, S.; Li, K.; Sun, X.; Xu, T.; and Chen, E. 2023. A Survey on Multimodal Large Language Models. *ArXiv*, abs/2306.13549.

Yoo, K. M.; Park, D.; Kang, J.; Lee, S.-W.; and Park, W. 2021. GPT3Mix: Leveraging Large-scale Language Models for Text Augmentation. In *Conference on Empirical Methods in Natural Language Processing*.

Zhang, H.; Li, X.; and Bing, L. 2023. Video-LLaMA: An Instruction-tuned Audio-Visual Language Model for Video Understanding. In *Conference on Empirical Methods in Natural Language Processing*.

Zhang, K.; Lv, A.; Chen, Y.; Ha, H.; Xu, T.; and Yan, R. 2024. Batch-ICL: Effective, Efficient, and Order-Agnostic In-Context Learning. *ArXiv*, abs/2401.06469.

Zhang, R.; Han, J.; Zhou, A.; Hu, X.; Yan, S.; Lu, P.; Li, H.; Gao, P.; and Qiao, Y. J. 2023a. LLaMA-Adapter: Efficient Fine-tuning of Language Models with Zero-init Attention. *ArXiv*, abs/2303.16199.

Zhang, Z.; Zhang, A.; Li, M.; Zhao, H.; Karypis, G.; and Smola, A. 2023b. Multimodal chain-of-thought reasoning in language models. *arXiv preprint arXiv:2302.00923*.

Zhao, W. X.; Zhou, K.; Li, J.; Tang, T.; Wang, X.; Hou, Y.; Min, Y.; Zhang, B.; Zhang, J.; Dong, Z.; Du, Y.; Yang, C.; Chen, Y.; Chen, Z.; Jiang, J.; Ren, R.; Li, Y.; Tang, X.; Liu, Z.; Liu, P.; Nie, J.; and rong Wen, J. 2023. A Survey of Large Language Models. *ArXiv*, abs/2303.18223.

Zhou, K.; Yang, J.; Loy, C. C.; and Liu, Z. 2021. Learning to Prompt for Vision-Language Models. *International Journal of Computer Vision*, 130: 2337 – 2348.

## Appendix

### A Task Constructions on OpenFlamingo

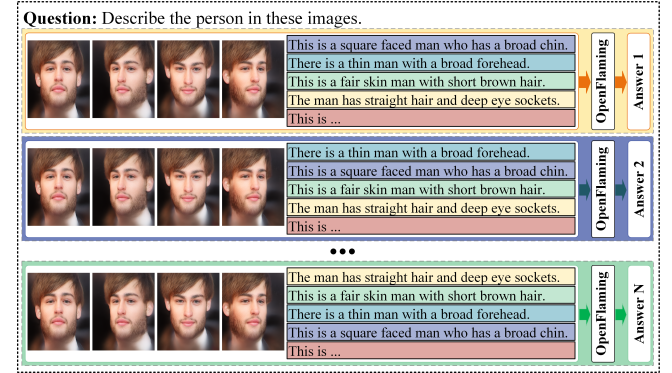


Figure 10: Description of text-only task on OpenFlamingo.

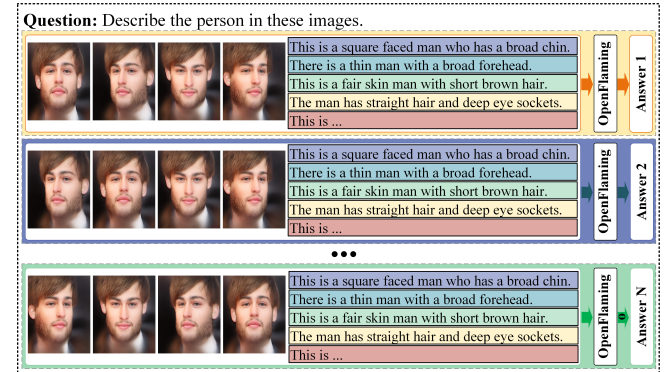


Figure 11: Description of image-only task on OpenFlamingo.

Here we present text-only and image-only tasks constructed using the CelebAText-HQ dataset (Sun et al. 2021). HFGI3D (Xie et al. 2022) is used to generate four distinct views of each facial image as visual prompts. For the text-only task, as shown in Figure 10, the order of facial image descriptions used as text prompts is altered in each experiment, while the order of facial images used as visual prompts remains constant. For the image-only task, as shown in Figure 11, conversely, the order of facial images used as visual prompts is changed in each experiment. In contrast, the order of facial image descriptions used as text prompts remains unchanged. The question is to describe the person in

the images. OpenFlamingo (Awadalla et al. 2023) is asked to generate answers based on each prompt order.

## B Task Constructions of Order Sensitivity

Here we present the details of task construction of order sensitivity. As shown in Figure 12. Text-only: Multiple-choice question-answering task, including a question related to an image and 4 text options. Image-only: Multiple-choice image-caption matching task, including a caption and 4 image options. Image-text-pair: Multiple-choice image-caption matching task, including 4 image-caption pair options.

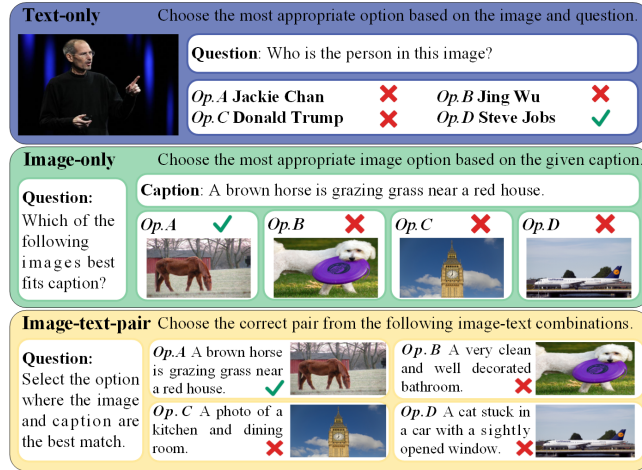


Figure 12: Tasks for order sensitivity.

## C Setup & Task Constructions of Experiment

The experiment utilizes an AMD EPYC 7H12 64-core processor as the CPU and four NVIDIA RTX A6000 Ada GPUs. The system has 256 GB of memory. The operating system is Ubuntu 22.04.3. The experiments use CUDA version 12.4. The software environments for the experiments vary depending on the project; specific configurations can be found in our technical appendix. For experiments involving Video-LLaVA, Python version 3.10.4 and torch version 2.0.1 are used. For other experiments, Python version 3.9.12 and torch version 2.1.2 are employed.

We present the details of task construction of the video-caption matching task and visual question answering task with RAG. As shown in Figure 13, *Key Frames* are placed at the front, middle, and back of the video, forming three comparative groups. The model is asked to answer questions separately. This allows us to verify whether the relative position of *Key Frames* in the video affects performance.

As shown in Figure 14, each question comes with a RAG image set containing 4 images, of which only one is the *Question-relevant image*. The *Question-relevant image* is placed in four different positions within the RAG image set, creating four comparative groups. The model is asked to answer questions separately. This allows us to verify whether the position of important content, i.e., the *Question-relevant image*, in the prompts from RAG, affects performance.

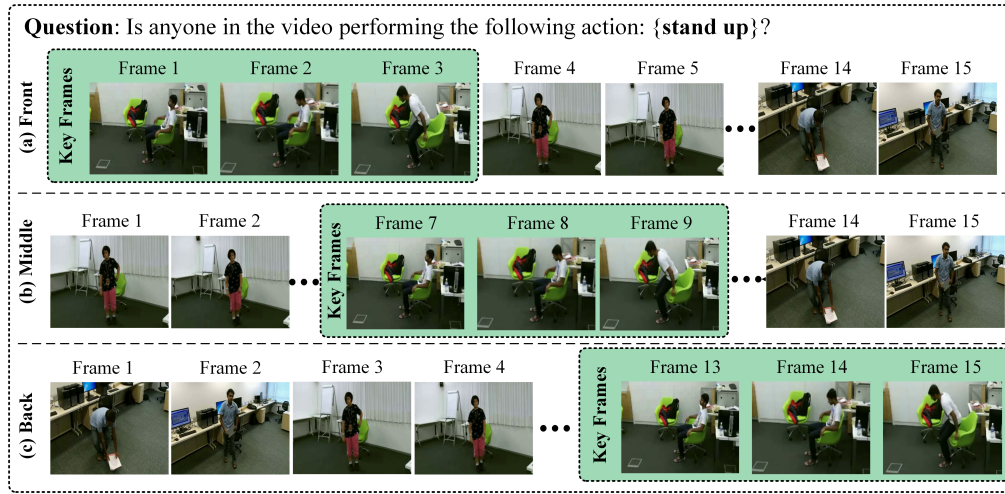


Figure 13: Demonstration of video-caption matching task.

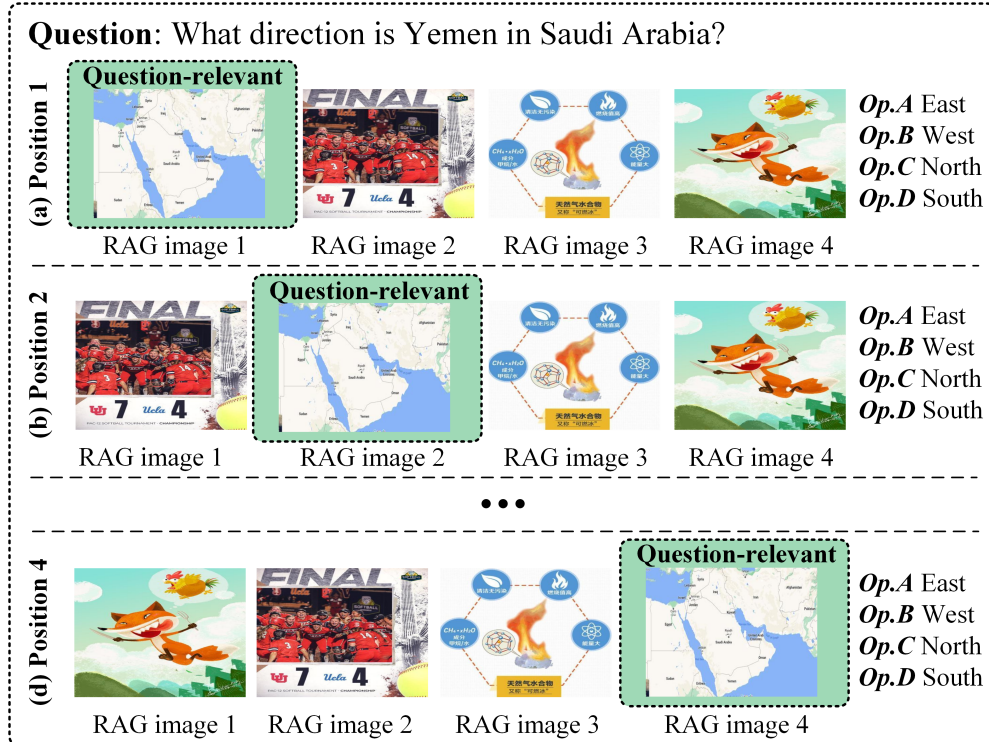


Figure 14: Demonstration of visual question answering task with RAG.